The Astrophysical Journal, 651:584–589, 2006 November 1

ON THE PHYSICAL REALIZATION OF TWO-DIMENSIONAL TURBULENCE FIELDS IN MAGNETIZED INTERPLANETARY PLASMAS

A. Stockem, I. Lerche, and R. Schlickeiser
Institut für Theoretische Physik, Lehrstuhl IV: Weltraum- und Astrophysik, Ruhr-Universität Bochum, D-44780 Bochum, Germany;
anne@tp4.rub.de, lercheian@yahoo.com, rsch@tp4.rub.de
Received 2006 April 26; accepted 2006 July 3

ABSTRACT

Studies of solar-flare cosmic-ray particle transport in the interplanetary medium and data analysis of the fluctuating solar wind magnetic fields have revealed the existence of dominating, two-dimensional transverse magnetic fluctuations. Here it is demonstrated that the filamentation instability of counterstreaming magnetized plasmas provides a plausible mechanism for the origin of this two-dimensional turbulence component. Solar coronal mass ejections into the interplanetary medium, as well as overtaking solar wind streams in the appropriate center of plasma mass reference system, correspond to energetic collisions of plasma shells with different nonrelativistic velocities. By analyzing the dispersion relation, it is shown that these plasma shell collisions quickly lead to the onset of purely growing aperiodic plasma instabilities perpendicular to the flow direction if the flow velocity difference is larger than $(1 + r_n)^{1/2}$ times the local Alfvén speed, where r_n denotes the density contrast of the colliding shells. For typical coronal mass ejections and parameters that allow overtaking the solar wind stream, the instability condition is well fulfilled, and the calculated growth rates of the fluctuations are short compared to the dynamical flare timescales.

Subject headings: cosmic rays — interplanetary medium — turbulence

1. INTRODUCTION

The data analysis of fluctuating solar wind magnetic fields assuming axisymmetric transverse fluctuations in a composite two-dimensional (2D) plus slab turbulence model (Bieber et al. 1996) revealed that as much as $\eta \sim 15\%$ of the fluctuation energy is associated with the slab component, while $(1 - \eta) \sim 85\%$ of the fluctuation energy comes from the 2D component. Such a dominating presence of the 2D component is also supported by numerical simulations regarding the cascading of nearly incompressible MHD turbulence (Montgomery & Turner 1981; Matthaeus et al. 1990). The advantage of viewing solar wind MHD turbulence as consisting of a superposition of a 2D component and a slab component was realized by Bieber et al. (1994) and Jaekel et al. (1994). Bieber et al. (1994) found good agreement between the mean free path inferred from solar particle events and theoretically calculated mean free paths λ predicted by slab quasi-linear transport theory if only $\eta \sim 15\%$ of the fluctuation energy is associated with the slab component. This result was based on the assumption that 2D turbulence does not contribute to cosmic-ray scattering. It was proved by Shalchi & Schlickeiser (2004) that 2D turbulence contributes much less effectively to cosmic-ray scattering, justifying the approximation $\lambda^{\eta} \simeq \lambda^{\rm slab}/\eta$ of the composite model (Bieber et al. 1994; Dröge 2003).

It is the purpose of the present investigation to propose a physical mechanism for the origin of the 2D turbulence component in magnetized cosmic plasmas based on the filamentation instability of counterstreaming plasmas. Flares in the solar wind are one prominent example of energetic collisions of plasma shells with different properties (temperature, density, composition, etc.). It is well known experimentally (Kapetanakos 1974; Tatarakis et al. 2003) and from numerous particle-in-cell (PIC) simulations (e.g., Lee & Lampe 1973; Nishikawa et al. 2003; Silva et al. 2003; Frederiksen et al. 2004; Sakai et al. 2004; Jaroschek et al. 2005) that such collisions lead to the onset of linear plasma instabilities perpendicular to the flow directions both in unmagnetized and slightly magnetized plasmas and subsequently to the development of nonlinear filamentary structures. In the center of the plasma mass system, the colliding shells can be described as two interpenetrating collisionless particle streams of different densities and speeds. The resulting filamentation is a manifestation of the Biot-Savart attractive current-current interaction between stream particles that can predominate over the dynamics when the plasma shields out electrostatic interactions (Molvig 1975).

In the case of unmagnetized plasmas, the filamentation instability has been proposed as a mechanism to magnetize the early universe (Gruzinov 2001; Okabe & Hattori 2003; Schlickeiser & Shukla 2003; Schlickeiser 2005), the pulsar wind nebula at the termination of pulsar winds (Gallant et al. 1992), and γ-ray burst sources (Medvedev & Loeb 1999). Physically, the instability is similar to a two-stream instability in which the relative motion between two interpenetrating electron streams generates currents that are the source of the magnetic field. This magnetic field generation process sets in when the streaming velocity exceeds a critical threshold speed. When the spatial scale of the excited fields is of the order of the electron gyroradius, the magnetic fields saturate at subequipartition levels due to the magnetic trapping of electrons in the wave potential.

The treatment of the filamentation instability in initially magnetized anisotropic plasmas is theoretically much more involved due to longitudinal and transverse mode-coupling effects. It is known experimentally (Kapetanakos 1974) that a strong enough guiding magnetic field inhibits the filamentation instability. This result is supported by PIC simulations of two-stream instabilities in the presence of ambient magnetic fields (Hededal & Nishikawa 2005). Molvig (1975) showed that in an electron plasma, a beam with bulk velocity βc is stabilized if the nonrelativistic electron gyrofrequency $\Omega_{\rm ce} > \omega_b \beta (1 - \beta^2)^{-1/2}$ regardless of its temperature, where ω_b denotes the electron beam plasma frequency.

Here for the case of magnetized four-stream instabilities of overall neutral electron-proton or electron-positron streams, we derive the critical magnetic field strength B_c, above which the filamentation instability is inhibited, in terms of the streaming speeds and the local plasma parameters. The critical field strength B_c is then calculated for typical interplanetary and solar-flare streaming conditions. Significant 2D turbulence can be generated by the filamentation instability only if the ambient magnetic field strength is smaller than the critical field ($B_0 < B_c$). In addition, in the case of solar flares, the minimum growth time has to be smaller than the flare duration.

2. MAGNETIZED NEUTRAL FOUR-STREAM INSTABILITIES

We consider a plasma system consisting of two cold streams ($i = 1$ and 2), each consisting of an equal number of positively and negatively charged particles, moving with different velocities U_i along an ordered magnetic field. The total gyrotropic particle distribution function is

$$f(p_\perp, p_\|) = \frac{\delta(p_\perp)}{2\pi p_\perp}\Big[N_1\delta(p_\| - \Gamma_1 m_+ U_1) + N_1\delta(p_\| - \Gamma_1 m_- U_1) + N_2\delta(p_\| + \Gamma_2 m_+ U_2) + N_2\delta(p_\| + \Gamma_2 m_- U_2)\Big], \tag{1}$$

where $\Gamma_i = [1 - (U_i/c)^2]^{-1/2}$.

Because of the assumption of an equal number of positively and negatively charged particles, no restrictions apply to the values of N_1, N_2, U_1, and U_2 in order to avoid large-scale charge and current densities. In this respect, our distribution function (1) differs from previous investigations that have assumed either one counterstreaming plasma component traversing a second plasma component at rest (Lee 1969), an electron beam along a magnetic guide field in a charge- and current-neutralized two-temperature Maxwellian plasma (Molvig 1975), or plasma streams with equal densities $N_1 = N_2$ (Lee 1970; Shivamoggi 1982; Saito & Sakai 2004). The neutral four-stream instability investigated here is closely related to the so-called electromagnetic counterstreaming instability (Saito & Sakai 2004; Medvedev & Loeb 1999), with the anisotropic temperatures replaced here by cold particle beams. This configuration is often referred to as an extreme form of temperature anisotropy (Jaroschek et al. 2005). The cold plasma approximations in equation (1) have been chosen mainly for mathematical convenience; they allow a straightforward analytical analysis of the instability conditions from inspecting a polynomial dispersion relation (see below). An extension of the analysis to nonzero temperatures would be a more realistic representation of the interplanetary environment. However, the respective dispersion relation of perpendicular waves in counterstreaming Maxwellian plasmas (Tautz & Schlickeiser 2006, eqs. [14] and [15]) involves the regularized hypergeometric function ${}_2F_2$, and the instability analysis becomes less transparent.

A second argument to justify the chosen extreme form of temperature anisotropy of equation (1) comes from the work of Molvig (1975), who, for an electron plasma with thermal dispersion, demonstrated that the stability condition is independent of the electron temperature. A corresponding temperature independence for multicomponent plasmas, therefore, is likely, although not guaranteed.

2.1. *General Dispersion Relation*

The distribution function (1) implies nine elements of the dielectric tensor (Schlickeiser 2002, p. 212; Melrose 1980, p. 59). In the case of wave propagation perpendicular to the ordered magnetic field ($k_\| = 0$), one has

$$\psi_{11} = \psi_{22} = 1 - \sum_{n=1,2}\frac{(1+\chi)\omega_{\rm pn}^2}{\Gamma_n} \times \frac{\omega^2 - (\chi\Omega^2/\Gamma_n^2)}{[\omega^2 - (\Omega^2/\Gamma_n^2)][\omega^2 - (\chi^2\Omega^2/\Gamma_n^2)]},$$

$$\psi_{33} = 1 - \sum_{n=1,2}\frac{(1+\chi)\omega_{\rm pn}^2}{\omega^2\Gamma_n^3} - \frac{k_\perp^2}{\omega^2}\sum_{n=1,2}\frac{(1+\chi)\omega_{\rm pn}^2 U_n^2}{\Gamma_n} \times \frac{\omega^2 - (\chi\Omega^2/\Gamma_n^2)}{[\omega^2 - (\Omega^2/\Gamma_n^2)][\omega^2 - (\chi^2\Omega^2/\Gamma_n^2)]},$$

$$\psi_{12} = -\psi_{21} = iD,$$

with

$$D = (1-\chi^2)\omega\sum_{n=1,2}\frac{\omega_{\rm pn}^2\Omega}{\Gamma_n^2[\omega^2 - (\Omega^2/\Gamma_n^2)][\omega^2 - (\chi^2\Omega^2/\Gamma_n^2)]},$$

$$\psi_{13} = \psi_{31} = \frac{k_\perp}{\omega}\sum_{n=1,2}\frac{(1+\chi)\omega_{\rm pn}^2 U_n}{\Gamma_n} \times \frac{\omega^2 - (\chi\Omega^2/\Gamma_n^2)}{[\omega^2 - (\Omega^2/\Gamma_n^2)][\omega^2 - (\chi^2\Omega^2/\Gamma_n^2)]},$$

$$\psi_{23} = -\psi_{32} = -ik_\perp\Omega(1-\chi^2) \times \sum_{n=1,2}\frac{\omega_{\rm pn}^2 U_n}{\Gamma_n^2[\omega^2 - (\chi^2\Omega^2/\Gamma_n^2)][\omega^2 - (\Omega^2/\Gamma_n^2)]},$$

the nonrelativistic electron gyrofrequencies $\Omega = eB_0/m_- c$, the nonrelativistic electron plasma frequencies $\omega_{\rm pn} = (4\pi e^2 N_n/m_-)^{1/2}$, and the mass ratio $\chi = m_-/m_+$.

For the Maxwell operator, we then obtain (with $k = k_\perp$)

$$\Lambda_{ij} = \psi_{ij} - \left(\frac{kc}{\omega}\right)^2(\delta_{33} + \delta_{22}) = \begin{pmatrix} \psi_{11} & iD & \psi_{13} \\ -iD & \psi_{11} - \left(\frac{kc}{\omega}\right)^2 & \psi_{23} \\ \psi_{13} & -\psi_{23} & \psi_{33} - \left(\frac{kc}{\omega}\right)^2 \end{pmatrix}, \tag{2}$$

so that the dispersion relation $\det \Lambda_{ij} = 0$ in this general case yields a polynomial equation of the sixth order in ω^2. Simplification factorization occurs under the following restrictions:

1. For equal mass flows, such as pair flows, the mass ratio is $\chi = 1$, so that $D = 0$ and $\psi_{23} = 0$ throughout, and the dispersion relation factors as

$$0 = \left[\psi_{11} - \left(\frac{kc}{\omega}\right)^2\right]\left\{\psi_{11}\left[\psi_{33} - \left(\frac{kc}{\omega}\right)^2\right] - \psi_{13}^2\right\}. \tag{3}$$

2. For symmetric, counterstreaming flows $U_2 = -U_1$, implying $\Gamma_1 = \Gamma_2$, one has $\psi_{13} = 0$, leaving

$$0 = \left[\psi_{33} - \left(\frac{kc}{\omega}\right)^2\right]\left[\psi_{11}^2 - D^2 - \left(\frac{kc}{\omega}\right)^2 \psi_{11}\right]. \quad (4)$$

3. An even simpler form results for symmetric counterstreaming pair plasmas,

$$0 = \left[\psi_{33} - \left(\frac{kc}{\omega}\right)^2\right]\left[\psi_{11} - \left(\frac{kc}{\omega}\right)^2\right]\psi_{11}. \quad (5)$$

In the following we consider nonrelativistic flows $U_i \ll c$, appropriate for solar flares and many interstellar applications.

2.2. *Nonrelativistic Flows*

For nonrelativistic flows $U_i \ll c$, so that $\Gamma_i \simeq 1$, which is appropriate for solar flares, we obtain

$$\begin{aligned}\psi_{13} = \psi_{31} &\simeq \frac{k}{\omega}(1+\chi)\frac{\omega^2 - \chi\Omega^2}{(\omega^2 - \Omega^2)(\omega^2 - \chi^2\Omega^2)}\sum_{n=1,2}\omega_{\mathrm{p}n}^2 U_n \\ &= \frac{k}{\omega}(1+\chi)\frac{4\pi e^2}{m_-}\frac{\omega^2 - \chi\Omega^2}{(\omega^2 - \Omega^2)(\omega^2 - \chi^2\Omega^2)}\sum_{n=1,2} N_n U_n, \quad (6)\end{aligned}$$

$$\begin{aligned}\psi_{23} &= -\frac{ik\Omega(1-\chi^2)}{(\omega^2 - \Omega^2)(\omega^2 - \chi^2\Omega^2)}\sum_{n=1,2}\omega_{\mathrm{p}n}^2 U_n \\ &= -\frac{ik\Omega(1-\chi^2)}{(\omega^2 - \Omega^2)(\omega^2 - \chi^2\Omega^2)}\frac{4\pi e^2}{m_-}\sum_{n=1,2} N_n U_n, \quad (7)\end{aligned}$$

In the plasma mass center system, the condition $N_1(m_+ + m_-)U_1 + N_2(m_+ + m_-)U_2 = 0$ holds, yielding the constraint

$$N_1 U_1 + N_2 U_2 = \sum_{n=1,2} N_n U_n = 0, \quad (8)$$

so that equations (6) and (7) reduce to $\psi_{13} = 0$ and $\psi_{23} = 0$, respectively. With respect to the observer's frame of reference, the center of the plasma mass system moves with velocity

$$V_c = \frac{\sum_{n=1,2} N_n(m_+ + m_-)u_n}{\sum_{n=1,2} N_n(m_+ + m_-)} = \frac{\sum_{n=1,2} u_n N_n}{\sum_{n=1,2} N_n}, \quad (9)$$

where u_i denotes the flow velocities in the observer's frame. For nonrelativistic flows, the Galilean velocity transformation is simply $U_i = u_i - V_c$, immediately yielding

$$U_1 = \frac{(u_1 - u_2)N_2}{N_1 + N_2}, \quad U_2 = \frac{(u_2 - u_1)N_1}{N_1 + N_2}, \quad (10)$$

which satisfy condition (8).

In the center of the plasma mass system, the dispersion relation then becomes

$$0 = \left[\Psi_{33} - \left(\frac{kc}{\omega}\right)^2\right]\left\{\Psi_{11}\left[\Psi_{11} - \left(\frac{kc}{\omega}\right)^2\right] - D_c^2\right\}, \quad (11)$$

with

$$\Psi_{11} \simeq 1 - \sum_{n=1,2}(1+\chi)\omega_{\mathrm{p}n}^2\frac{\omega^2 - \chi\Omega^2}{(\omega^2 - \Omega^2)(\omega^2 - \chi^2\Omega^2)},$$

$$\begin{aligned}\Psi_{33} \simeq 1 &- \sum_{n=1,2}\frac{(1+\chi)\omega_{\mathrm{p}n}^2}{\omega^2} \\ &- \frac{k^2}{\omega^2}\sum_{n=1,2}(1+\chi)\omega_{\mathrm{p}n}^2 U_n^2\frac{\omega^2 - \chi\Omega^2}{(\omega^2 - \Omega^2)(\omega^2 - \chi^2\Omega^2)},\end{aligned}$$

$$D_c = (1-\chi^2)\omega\sum_{n=1,2}\frac{\omega_{\mathrm{p}n}^2\Omega}{(\omega^2 - \Omega^2)(\omega^2 - \chi^2\Omega^2)}.$$

The dispersion relation (11) factorizes into the two modes

$$\Psi_{11}\left[\Psi_{11} - \left(\frac{kc}{\omega}\right)^2\right] - D_c^2 = 0, \quad (12)$$

$$\Psi_{33} = \left(\frac{kc}{\omega}\right)^2. \quad (13)$$

The last mode (eq. [13]) includes the filamentation instability and reads

$$\begin{aligned}k^2c^2 = \omega^2 &- (1+\chi)\sum_{n=1,2}\omega_{\mathrm{p}n}^2 \\ &- (1+\chi)k^2\frac{\omega^2 - \chi\Omega^2}{(\omega^2 - \Omega^2)(\omega^2 - \chi^2\Omega^2)}\sum_{n=1,2}\omega_{\mathrm{p}n}^2 U_n^2. \quad (14)\end{aligned}$$

It is appropriate to introduce the density ratio $r_n = N_1/N_2$ and the total plasma frequency

$$\begin{aligned}\omega_p^2 &= (1+\chi)\sum_{n=1,2}\omega_{\mathrm{p}n}^2 \\ &= (1+\chi)\omega_{p1}^2\left(1 + \frac{N_2}{N_1}\right) = (1+\chi)\omega_{p1}^2\frac{1+r_n}{r_n}. \quad (15)\end{aligned}$$

Then equation (8) yields

$$(1+\chi)\sum_{n=1,2}\omega_{\mathrm{p}n}^2 U_n^2 = r_n\omega_p^2 U_1^2.$$

The dispersion relation (14) then becomes

$$0 = \omega^2 - \omega_p^2 - k^2c^2 - \omega_p^2 r_n U_1^2 k^2\frac{\omega^2 - \chi\Omega^2}{(\omega^2 - \Omega^2)(\omega^2 - \chi^2\Omega^2)}, \quad (16)$$

yielding the cubic dispersion relation

$$M(f) = f^3 - Af^2 + Gf - C = 0, \quad (17)$$

with $f = \omega^2$,

$$A = \omega_p^2 + k^2c^2 + (1+\chi^2)\Omega^2 > 0, \quad (18a)$$

$$G = \chi^2\Omega^4 + (1+\chi^2)\Omega^2\left(\omega_p^2 + k^2c^2\right) - \omega_p^2 r_n k^2 U_1^2, \quad (18b)$$

$$C = \chi\Omega^2\left[\chi\Omega^2\left(\omega_p^2 + k^2c^2\right) - \omega_p^2 r_n k^2 U_1^2\right]. \quad (18c)$$

In the case of an electron-proton plasma with density ratio $r_n = 1$, dispersion relation (16) agrees with equation (6) of Lee (1970) for equal proton and electron speeds $U_p = U_e$, as assumed here.

2.3. *Condition for Aperiodic Fluctuations*

We write k^2c^2 in dispersion relation (16) as a function of ω^2, i.e.,

$$k^2c^2 = \frac{\omega^2 - \omega_p^2}{1 + \omega_p^2 r_n (U_1/c)^2 \left[(\omega^2 - \chi\Omega^2)/(\omega^2 - \Omega^2)(\omega^2 - \chi^2\Omega^2)\right]},$$

and investigate aperiodic fluctuations characterized by $\omega^2 = -\sigma^2$. In this case, one of the solutions, $\pm\sigma$, leads to purely growing aperiodic fluctuations with zero real part of the frequency ($\omega_R = i\sigma$). Scale $\sigma^2 = x\Omega^2$ to obtain

$$\frac{k^2c^2}{\Omega^2} = F(x) = -\frac{(x+\alpha)(x+\chi^2)(x+1)}{(x+\chi^2)(x+1) - g(x+\chi)}, \quad (19)$$

with $\alpha = (\omega_p/\Omega)^2$ and $g = \alpha r_n (U_1/c)^2$. Aperiodic solutions with purely imaginary frequency ω and real wavenumber k result if x and $F(x)$ are positive. We limit our analysis here to electron-proton plasmas with $\chi = 1/1836$.

Obviously,

$$F(x) = -\frac{Z(x)}{N(x)}. \quad (20)$$

For $x > 0$, the numerator $Z(x)$ is always positive. The denominator is a second-order function with a minimum at

$$x_{\min} = -\frac{1}{2}(\chi^2 + 1 - g), \quad (21)$$

$$N_{\min}(x) = -\frac{1}{4}(\chi^2 + 1 - g)^2 + \chi(\chi - g). \quad (22)$$

There are two cases:

1. $g < \chi^2 + 1 \Leftrightarrow x_{\min} < 0$: for $x > 0 > x_{\min}$, the derivation dN/dx is positive. Hence, $N(x) > N(0) = \chi(\chi - g)$.
   (*a*) $g < \chi$: $N(x)$ is positive and there exist no positive roots.
   (*b*) $\chi \leq g \leq \chi^2 + 1$: $N(0) < 0$. Positive roots are possible.
2. $g > \chi^2 + 1 \Leftrightarrow x_{\min} > 0$: with equation (22) the minimum becomes negative and at least one positive root exists.

The condition for aperiodic solutions, therefore, reads $g > \chi$. Factorizing the denominator in equation (19) then yields

$$F(x) = -\frac{(x+\alpha)(x+\chi^2)(x+1)}{(x-x_1)(x+x_2)}, \quad (23)$$

with

$$x_1 = \frac{1}{2}\left[\sqrt{(g-1-\chi^2)^2 + 4\chi(g-\chi)} + (g-1-\chi^2)\right] > 0,$$

$$x_2 = -X_2 = \frac{1}{2}\left[\sqrt{(g-1-\chi^2)^2 + 4\chi(g-\chi)} - (g-1-\chi^2)\right] > 0.$$

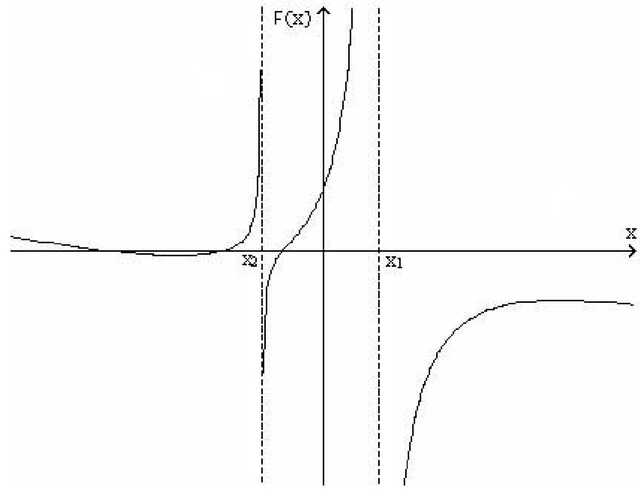

FIG. 1.—Sketch of the function $F(x)$.

For all $g > \chi$, the root x_1 is real and positive, whereas the root $-x_2$ is real and negative. For the function $F(x)$, this behavior causes one pole at the positive value x_1 and one pole at the negative value $-x_2$. The function $F(x) > 0$ in the range $0 \leq x \leq x_1$ (see Fig. 1). A minimum wavenumber for aperiodic fluctuations results at $x = 0$,

$$k^2 > k_{\min}^2 = \frac{\Omega^2}{c^2}F(0) = \frac{\Omega^2}{c^2}\frac{\alpha\chi}{g-\chi} = \frac{\omega_p^2}{c^2}\frac{1}{(g/\chi)-1} = \frac{\omega_p^2}{\left[\left(\omega_p^2 r_n U_1^2\right)/\left(\chi\Omega^2\right)\right] - c^2}, \quad (24)$$

corresponding to spatial scales

$$L < L_{\max} = \frac{2\pi}{k_{\min}} = 2\pi\frac{c}{\omega_p}\sqrt{\frac{g}{\chi} - 1}. \quad (25)$$

For large values $g/\chi = 1836g \gg 1$, the maximum scale can be approximated by

$$L_{\max} = 270\frac{r_n^{1/2}U_1}{\Omega} = 270\frac{r_n^{1/2}|u_1 - u_2|}{(1+r_n)\Omega}\ \text{cm}, \quad (26)$$

scaling inversely proportional to the ordered magnetic field value.

2.4. *Instability Conditions*

In order to have nonnegative values of $k_{\min}^2$ in equation (24), the streaming velocity threshold is

$$U_1^2 \geq \frac{\chi\Omega^2c^2}{r_n\omega_p^2}. \quad (27)$$

The threshold condition (26) together with equation (10a) gives an upper limit for the magnetic field strength $B \leq B_c$,

$$B_c = \frac{m_-}{e}\sqrt{\frac{r_n}{\chi}}\omega_p|U_1| = \frac{m_-}{e}\sqrt{\frac{1+\chi}{\chi(1+r_n)}}\omega_{p1}|u_1 - u_2|. \quad (28)$$

In terms of the Alfvén speed,

$$V_{A1} = \frac{B}{\sqrt{4\pi N_1(m_- + m_+)}} = \sqrt{\frac{\chi}{1+\chi}}\frac{\Omega c}{\omega_{p1}} = \sqrt{\chi\frac{1+r_n}{r_n}}\frac{\Omega c}{\omega_p},$$

the threshold condition (27) reads

$$|u_1 - u_2| \geq V_{A1}\sqrt{1+r_n}. \quad (29)$$

For electron-proton flows, the critical magnetic field value in equation (28) is (with $u_i = \beta_i c$)

$$B_{c,\text{electron-proton}} = 0.138|\beta_1 - \beta_2|\frac{\sqrt{n_{e1}/1\ \text{cm}^{-3}}}{\sqrt{1+r_n}}\ \text{G} \quad (30)$$

2.5. *Growth Rate of Filamentation Instability*

In order to derive the growth rate σ of the aperiodic fluctuations we consider the two cases of (1) very large wavenumber values of $k^2 \to \infty$ and (2) wavenumbers slightly larger than $k^2_{\min}$. For large enough values of k^2, Figure 1 indicates that $x \simeq x_1$, implying the maximum growth rate for high wavenumbers,

$$\sigma_{\max} \simeq \Omega x_1^{1/2} = \frac{\Omega}{2^{1/2}}\left[\sqrt{(g-1-\chi^2)^2 + 4\chi(g-\chi)} + (g-1-\chi^2)\right]^{1/2} \simeq \Omega\left[\frac{\chi(g-\chi)}{1-g}\right]^{1/2}, \quad (31)$$

where the last approximation holds for $g \ll 1$. The maximum growth rate is independent of wavenumber.

For $x \ll x_1$, we Taylor expand function (23) to first order around $x = 0$, so that

$$F(x) \simeq F(0) + \left(\frac{dF}{dx}\Big|_{x=0}\right)x.$$

With equation (24) and

$$\frac{dF}{dx}\Big|_{x=0} = \frac{1}{\chi(g-\chi)^2}\left[\chi^2(g-\chi) + g\alpha(1+\chi^2-\chi)\right], \quad (32)$$

we obtain

$$x = \frac{\sigma^2}{\Omega^2} \simeq \frac{1}{dF/dx|_{x=0}}\left[\frac{c^2k^2}{\Omega^2} - \frac{c^2k^2_{\min}}{\Omega^2}\right],$$

yielding

$$\sigma \simeq c|g-\chi|\sqrt{\frac{\chi}{\chi^2(g-\chi) + g\alpha(1+\chi^2-\chi)}}\sqrt{k^2 - k^2_{\min}}. \quad (33)$$

3. APPLICATION TO SOLAR FLARES

We consider two applications in the interplanetary medium that are relevant for energetic particles. In each case we derive the plasma and outflow parameter for which the filamentation instability operates and calculate the spatial scale of the fluctuations together with the growth rate for aperiodic fluctuations.

3.1. *Solar Coronal Mass Ejections*

As a first application we consider solar flares that result from solar coronal mass ejections (CMEs). CMEs are a major form of eruptive phenomena in the solar corona involving masses of the order of $\simeq 10^{15}$–10^{16} g and kinetic energies of $\simeq 10^{30}$–10^{32} ergs. The leading-edge speeds of CMEs within about 5 $R_\odot$ of the surface range from less than 50 to greater than 2000 km s^{-1} (Howard et al. 1985; Benz 1993; Sheeley et al. 2000), with an estimated Alfvén speed of $V_{A1} = 400$ km s^{-1}. Adopting $B_0 = 0.01$ G, a density $N_1 = 3000$ cm^{-3} is implied for the outflow plasma. Here we represent this nonrelativistic outflow as an electron-proton outflow with $u_1 = 2000$ km s^{-1} and $N_1 = 3000$ cm^{-3}, overtaking the electron-proton interplanetary medium at rest ($u_2 = 0$).

According to condition (29), an unstable situation arises only if the density contrast $r_n \leq 24$, i.e., for an interplanetary electron density $N_2 \geq N_1/24 = 125$ cm^{-3}. Adopting $N_2 = 200$ cm^{-3}, i.e., $r_n = 15$, we find that the velocity of the plasma mass system in equation (9) in this case is $V_c = 1875$ km s^{-1}, yielding $U_1 = 125$ km s^{-1} and $U_2 = -1882$ km s^{-1} for the flow velocities in equation (10) in the plasma mass system. In this case the parameter ratio $g/\chi = 1.47$ yields the maximum growth rate in equation (31) of the filamentation instability as

$$\sigma_{\max} = 65.7(B_0/0.01\ \text{G})\ \text{Hz}. \quad (34)$$

The minimum growth time $\tau = \sigma^{-1}_{\max} = 0.015(B_0/0.01\ \text{G})^{-1}$ s is significantly shorter than any other dynamical CME or solar-flare timescale. According to equation (25), the spatial scales of the fluctuations are smaller than $L_{\max} = 4 \times 10^4$ cm.

3.2. *Overtaking Solar Wind Streams*

As a second application, we consider the overtaking of a slow electron-proton solar wind stream ($u_2 = 300$ km s^{-1}, $N_2 = 20$ cm^{-3}) by a fast electron-proton stream ($u_1 = 600$ km s^{-1}, $N_1 = 10$ cm^{-3}) with an interplanetary magnetic field of 10^{-4} G. In this case $V_{A1} = 69$ km s^{-1}, and the density contrast is $r_n = 0.5$. In this case, again the instability condition (24) is fulfilled because $|u_1 - u_2| = 300$ km s^{-1} is larger than $V_{A1}(1+r_n)^{1/2} = 85$ km s^{-1}.

In this example, the parameter $g/\chi = 12.53$, so that

$$\sigma_{\max} = 3.3(B_0/10^{-4}\ \text{G})\ \text{Hz}. \quad (35)$$

The minimum growth time $\tau = \sigma^{-1} = 0.3(B_0/10^{-4}\ \text{G})^{-1}$ s is sufficiently short compared to typical (of order several hours) long-duration solar-flare timescales. According to equation (26), in this case the spatial scales of the fluctuations are smaller than $L_{\max} = 2.2 \times 10^6$ cm.

4. SUMMARY AND CONCLUSIONS

Studies of the solar-flare cosmic-ray particle transport in the interplanetary medium and the data analysis of the fluctuating solar wind magnetic fields have revealed the existence of dominating two-dimensional transverse magnetic fluctuations. Here we demonstrated that the filamentation instability of counterstreaming magnetized plasmas provides a plausible mechanism for the origin of this 2D turbulence component. Solar coronal mass ejections into the interplanetary medium, as well as overtaking solar wind streams in the appropriate center of plasma mass reference system, correspond to energetic collisions of plasma shells with different nonrelativistic velocities.

Analyzing the dispersion relation we showed that these plasma shell collisions quickly lead to the onset of purely growing aperiodic plasma instabilities perpendicular to the flow directions. The instability threshold can be formulated in two equivalent conditions: either (1) the plasma magnetic field strength must be less than a critical field strength B_c given by the flow velocity differences (eq. [28]), or (2) the flow velocity difference must be larger than the local Alfvén speed times $(1 + r_n)^{1/2}$, where r_n denotes the density contrast of the colliding shells (eq. [29]). For typical coronal mass ejections and overtaking solar wind stream parameters, the instability conditions are well fulfilled, and the calculated growth rates of the fluctuations are short compared to the dynamical flare timescales. We have shown that the maximum spatial scale increases inversely proportional to the strength of the ordered magnetic field. The relatively large values of the ordered magnetic field in the two applications discussed limit the spatial scales of the aperiodic fluctuations to 4×10^4 and 2×10^6 cm, respectively. Larger spatial scales would result for smaller guiding magnetic field strengths. Therefore, our results are consistent with studies of the filamentation instability without guiding ordered magnetic fields where no limiting restrictions on the maximum fluctuation scale result. It appears that a viable physical realization of the 2D turbulence fields has been established.

We thank the referee for constructive comments. This work is supported by the Deutsche Forschungsgemeinschaft through the Sonderforschungsbereich 591, through grant Schl 201/17-1 and through the award of a Mercator Professorship to one of the authors (I. L.).

REFERENCES

Benz, A. O. 1993, Plasma Astrophysics: Kinetic Processes in Solar and Stellar Coronae (Dordrecht: Kluwer)
Bieber, J. W., Matthaeus, W. H., Smith, C. W., Wanner, W., Kallenrode, M.-B., & Wibberenz, G. 1994, ApJ, 420, 294
Bieber, J. W., Wanner, W., & Matthaeus, W. H. 1996, J. Geophys. Res., 101, 2511
Dröge, W. 2003, ApJ, 589, 1027
Frederiksen, J. T., Hededal, C. B., Haugbølle, T., & Nordlund, A., 2004, ApJ, 608, L13
Gallant, Y., Hoshino, M., Langdon, A. B., Arons, J., & Max, C. E. 1992, ApJ, 391, 73
Gruzinov, A. 2001, ApJ, 563, L15
Hededal, C. B., & Nishikawa, K.-I. 2005, ApJ, 623, L89
Howard, R. A., Sheeley, N. R., Koomen, M. J., & Michels, D. J. 1985, J. Geophys. Res., 90, 8173
Jaekel, U., Wanner, W., Schlickeiser, R., & Wibberenz, G. 1994, A&A, 291, L35
Jaroschek, C. H., Lesch, H., & Treumann, R. A. 2005, ApJ, 618, 822
Kapetanakos, C. A. 1974, Appl. Phys. Lett., 25, 484
Lee, K. F. 1969, Phys. Rev., 181, 447
———. 1970, J. Appl. Phys., 41, 3045
Lee, R., & Lampe, M. 1973, Phys. Rev. Lett., 31, 1390
Matthaeus, W. H., Goldstein, M. L., & Roberts, D. A. 1990, J. Geophys. Res., 95, 20673
Medvedev, M., & Loeb, A. 1999, ApJ, 526, 697
Melrose, D. B. 1980, Plasma Astrophysics, Vol. 1 (New York: Gordon & Breach)
Molvig, K. 1975, Phys. Rev. Lett., 35, 1504
Montgomery, D., & Turner, L. 1981, Phys. Fluids, 24, 825
Nishikawa, K.-I., Hardee, P., Richardson, G., Preece, R., Sol, H., & Fishman, G. J. 2003, ApJ, 595, 555
Okabe, N., & Hattori, M. 2003, ApJ, 599, 964
Saito, S., & Sakai, J.-I. 2004, Phys. Plasmas, 11, 859
Sakai, J.-I., Schlickeiser, R., & Shukla, P. K. 2004, Phys. Lett. A, 330, 384
Schlickeiser, R. 2002, Cosmic Ray Astrophysics (Heidelberg: Springer)
———. 2005, Plasma Phys. Controlled Fusion, 47, A205
Schlickeiser, R., & Shukla, P. K. 2003, ApJ, 599, L57
Shalchi, A., & Schlickeiser, R. 2004, ApJ, 604, 861
Sheeley, N. R., Hakala, W. N., & Wang, Y.-M. 2000, J. Geophys. Res., 105, 5081
Shivamoggi, B. K. 1982, Ap&SS, 83, 177
Silva, L. O., Fonseca, R. A., Tonge, J. W., Dawson, J. M., Mori, W. B., & Medvedev, M. 2003, ApJ, 596, L121
Tatarakis, M., et al. 2003, Phys. Rev. Lett., 90, 175001
Tautz, R., & Schlickeiser, R. 2006, Phys. Plasmas, 13, 062901